

AD _____

Award Number: DAMD17-02-1-0134

TITLE: Biomarkers of Selenium Chemoprevention of Prostate Cancer

PRINCIPAL INVESTIGATOR: Yan Dong, Ph.D.

CONTRACTING ORGANIZATION: Health Research, Incorporated
Buffalo, New York 14263

REPORT DATE: January 2003

TYPE OF REPORT: Annual Summary

PREPARED FOR: U.S. Army Medical Research and Materiel Command
Fort Detrick, Maryland 21702-5012

DISTRIBUTION STATEMENT: Approved for Public Release;
Distribution Unlimited

The views, opinions and/or findings contained in this report are those of the author(s) and should not be construed as an official Department of the Army position, policy or decision unless so designated by other documentation.

20030617 090

REPORT DOCUMENTATION PAGE

Form Approved
OMB No. 074-0188

Public reporting burden for this collection of information is estimated to average 1 hour per response, including the time for reviewing instructions, searching existing data sources, gathering and maintaining the data needed, and completing and reviewing this collection of information. Send comments regarding this burden estimate or any other aspect of this collection of information, including suggestions for reducing this burden to Washington Headquarters Services, Directorate for Information Operations and Reports, 1215 Jefferson Davis Highway, Suite 1204, Arlington, VA 22202-4302, and to the Office of Management and Budget, Paperwork Reduction Project (0704-0188), Washington, DC 20503

1. AGENCY USE ONLY (Leave blank)		2. REPORT DATE January 2003	3. REPORT TYPE AND DATES COVERED Annual Summary (1 Jan 02 - 31 Dec 02)	
4. TITLE AND SUBTITLE Biomarkers of Selenium Chemoprevention of Prostate Cancer			5. FUNDING NUMBERS DAMD17-02-1-0134	
6. AUTHOR(S) : Yan Dong, Ph.D.				
7. PERFORMING ORGANIZATION NAME(S) AND ADDRESS(ES) Health Research, Incorporated Buffalo, New York 14263 E-Mail: yan.dong@roswellpark.org			8. PERFORMING ORGANIZATION REPORT NUMBER	
9. SPONSORING / MONITORING AGENCY NAME(S) AND ADDRESS(ES) U.S. Army Medical Research and Materiel Command Fort Detrick, Maryland 21702-5012			10. SPONSORING / MONITORING AGENCY REPORT NUMBER	
11. SUPPLEMENTARY NOTES				
12a. DISTRIBUTION / AVAILABILITY STATEMENT Approved for Public Release; Distribution Unlimited				12b. DISTRIBUTION CODE
13. Abstract (Maximum 200 Words) (abstract should contain no proprietary or confidential information) The purpose of the present study was to examine the mechanism of selenium growth inhibition in PC-3 human prostate cancer cells. Selenium retarded cell cycle progression at multiple transition points without changing the proportion of cells in different phases of the cell cycle. Selenium treatment also resulted in a marked induction of apoptosis. Array analysis was then applied to profile the gene expression changes mediating selenium-induced growth inhibition. A large number of potential selenium-responsive genes that are diverse in biological functions were identified. These genes fell into 12 clusters of distinct kinetics of modulation by selenium. The expression changes of 10 genes critically involved in cell cycle regulation were selected for verification by Western analysis. An agreement rate of 70% was obtained from these confirmation experiments. The array data enabled us to focus on the role of potential key genes (e.g., GADD153, CHK2, and p21 ^{WAF1}) in initiating the action of selenium, as well as to propose tentative signaling pathways that are integral to the downstream effects of these genes. The data also provide valuable insights into novel biological effects of selenium, such as inhibition of cell invasion, initiation of DNA repair, and induction of TGF- β signaling.				
14. SUBJECT TERMS: selenium-responsive biomarkers, microarray analysis, mechanism of selenium chemoprevention				15. NUMBER OF PAGES 13
				16. PRICE CODE
17. SECURITY CLASSIFICATION OF REPORT Unclassified	18. SECURITY CLASSIFICATION OF THIS PAGE Unclassified	19. SECURITY CLASSIFICATION OF ABSTRACT Unclassified	20. LIMITATION OF ABSTRACT Unlimited	

Table of Contents

Cover.....	1
SF 298.....	2
Summary.....	4
Key Research Accomplishments.....	4
Reportable Outcomes.....	5
Appendices.....	6 - 13

Summary:

A major goal of this project is to identify suitable biomarkers of selenium chemoprevention in human prostate cell models. During this first year of funding period, we investigated the cellular and molecular changes mediated by selenium in the PC-3 human prostate cancer cell line. Please see the attached article (Dong *et al.*, Cancer Res., 63, 52-59) in Appendix for detailed description of the specific aspects of the research. In the original Statement of Work, we proposed to look at the normal prostate cells and the LNCaP prostate cancer cell line in the first year and the PC-3 cell line in the second year. The reason that we switched the sequence of the work is that PC-3 cells are relatively easy to handle. We would like to work out the experimental conditions first with this cell line before we proceed to the other two cell models.

Key Accomplishments:

- Selenium-induced growth inhibition in PC-3 cells is achieved mainly by cell cycle blockade coupled to an induction of apoptosis.
- A large variety of potential selenium-responsive genes were identified by oligonucleotide array analysis.
- Clustering analysis grouped these genes into early, intermediate, and late responsive clusters.
- Since early responsive genes may be important in initiating the cascade of events leading to the action of selenium, we classified these genes according to their known functions in cell growth and tumorigenesis. These include cell cycle regulators, apoptosis controllers, cell adhesion and invasion proteins, signaling molecules, transcription factors, and oncogenes/tumor suppressors.
- The expression changes of 10 genes critically involved in cell cycle regulation were selected for verification by Western analysis. An agreement rate of 70% was obtained from these confirmation experiments.
- From the array data, we were able to formulate a schematic diorama of signaling pathways that provide the supportive framework for understanding selenium-mediated cell cycle blockade.
- The data also provided valuable insights into novel biological effects of selenium, such as inhibition of cell invasion, initiation of DNA repair, and induction of TGF- β signaling.

Reportable Outcomes:

➤ **Publication:**

Dong, Y., Zhang, H., Hawthorn, L., Ganther, H.E., and Ip, C. (2003) Delineation of the molecular basis for selenium-induced growth arrest in human prostate cancer cells by oligonucleotide array. *Cancer Res.*, 63, 52-59.

➤ **Abstract:**

Dong, Y., Zhang, H., Hawthorn, L., and Ip, C. (2002) Delineation of the Molecular Basis for Selenium-induced Growth Arrest in Human Prostate Cancer Cells by Oligonucleotide Array. *Proceedings of the American Association for Cancer Research*, 43: 167

➤ **Presentation:**

93rd Annual Meeting of American Association for Cancer Research, April 2002, San Francisco, California. Poster Presentation, "Delineation of the Molecular Basis for Selenium-induced Growth Arrest in Human Prostate Cancer Cells by Oligonucleotide Array", Dong Y., Zhang, H., Hawthorn, L., and Ip C.

➤ **Employment received:**

Affiliate Member, Dept. of Cancer Chemoprevention, Roswell Park Cancer Institute, Buffalo, NY 14263

Delineation of the Molecular Basis for Selenium-induced Growth Arrest in Human Prostate Cancer Cells by Oligonucleotide Array¹

Yan Dong, Haitao Zhang, Lesleyann Hawthorn, Howard E. Ganther, and Clement Ip²

Departments of Cancer Prevention [Y. D., C. I.], and Cancer Genetics [H. Z., L. H.], Roswell Park Cancer Institute, Buffalo, New York 14263, and Department of Nutritional Sciences, University of Wisconsin, Madison, Wisconsin 53706 [H. E. G.]

ABSTRACT

Despite the growing interest in selenium intervention of prostate cancer in humans, scanty information is currently available on the molecular mechanism of selenium action. Our past research indicated that methylseleninic acid (MSA) is an excellent reagent for investigating the anticancer effect of selenium *in vitro*. The present study was designed to examine the cellular and molecular effects of MSA in PC-3 human prostate cancer cells. After exposure to physiological concentrations of MSA, these cells exhibited a dose- and time-dependent inhibition of growth. MSA retarded cell cycle progression at multiple transition points without changing the proportion of cells in different phases of the cell cycle. Flow cytometric analysis of annexin V- and propidium iodide-labeled cells showed a marked induction of apoptosis by MSA. Array analysis with the Affymetrix human genome U95A chip was then applied to profile the gene expression changes that might mediate the effects of selenium. Gene profiling was done in a time course experiment (at 12, 24, 36, and 48 h) using synchronized cells. A large number of potential selenium-responsive genes with diverse biological functions were identified. These genes fell into 12 clusters of distinct kinetics pattern of modulation by MSA. The expression changes of 10 genes known to be critically involved in cell cycle regulation were selected for verification by Western analysis to determine the reliability of the array data. An agreement rate of 70% was obtained based on these confirmation experiments. The array data enabled us to focus on the role of potential key genes (e.g., *GADD153*, *CHK2*, *p21^{WAF1}*, *cyclin A*, *CDKI*, and *DHFR*) that might be targets of MSA in impeding cell cycle progression. The data also provide valuable insights into novel biological effects of selenium, such as inhibition of cell invasion, DNA repair, and stimulation of transforming growth factor β signaling. The present study demonstrates the utility of a genome-wide analysis to elucidate the mechanism of selenium chemoprevention.

INTRODUCTION

Recruitment to the National Cancer Institute-sponsored SELECT³ trial began in 2001. This is a Phase III, double-blind, placebo-controlled, 12-year trial designed to assess the effect of selenium and vitamin E, either individually or in combination, on the incidence of prostate cancer. The launching of this trial is largely driven by the milestone finding of Clark *et al.* (1) that selenized yeast supplementation was capable of significantly reducing the incidence of prostate (RR = 0.37), lung (RR = 0.54), and colon cancers (RR = 0.42). The SELECT protocol also

provides for the establishment of a repository for prostate biopsy tissue, blood cells, and plasma. These materials will be put aside for research discoveries in the future. One of the secondary objectives of the trial is to study cellular and molecular biomarkers using the banked samples and to delineate their relevance with respect to prostate carcinogenesis and drug effects (2). Despite the considerable public interest in the potential benefit of selenium chemoprevention of prostate cancer, scanty information is currently available on the molecular targets or the signaling mechanism underlying the anticancer action of selenium. Our present study was aimed at addressing this gap of knowledge with the use of a human prostate cancer cell line.

Se-Met is the selenium compound used in the SELECT. It is, however, not particularly suitable for mechanism studies in cell culture. The reason is that Se-Met needs to be metabolized primarily in the liver to a monomethylated intermediate for the expression of its anticancer activity (3-6), and epithelial tissues generally have a low capacity to generate a monomethylated selenium metabolite from Se-Met. Consequently, concentrations of Se-Met that are 20-100 times above physiological levels are necessary to cause growth inhibition in cultured cells. Excessively high concentrations of Se-Met could produce a spectrum of nonspecific effects that may not be related to the anticancer effect of selenium. To obviate this problem, a stable monomethylated selenium metabolite, MSA ($\text{CH}_3\text{SeO}_2\text{H}$), was developed specifically for *in vitro* studies (7). We found that premalignant human breast cell lines were sensitive to growth inhibition and cell cycle block by MSA at a concentration as low as 2.5 μM (8). In addition, Jiang *et al.* (9) recently reported that MSA induced apoptosis in DU-145 human prostate cancer cells at a concentration of 5 μM . Sinha *et al.* (10) also showed that with mouse mammary tumor cells, a 10-min exposure to 5 μM MSA was sufficient to cause a change in the expression of a handful of genes as detected by the Atlas mouse cDNA expression array. The concentration of selenium used in the above studies is within the physiological range of selenium in the circulation. As expected, MSA also has excellent anticancer activity *in vivo* (7). We are, therefore, confident that the information obtained with MSA from cell culture studies would be relevant to the action of selenium.

In this study, we first examined the dose-dependent effect of MSA on the growth of the PC-3 human prostate cancer cell line. We then showed that growth inhibition by MSA was likely attributable to a combined effect on cell cycle block and apoptosis. Next we used the oligonucleotide array technology to gain further insight into the gene expression changes that might play a role in the regulation of these cellular events. Many potential selenium-responsive genes were identified by this method. These genes fell into 12 clusters of distinct kinetics pattern of modulation by MSA. The early response genes were grouped on the basis of their known functions in cell growth and tumorigenesis. From the array data, we were able to develop an integrated scheme of signaling pathways that might explain the action of selenium in blocking cell cycle progression.

MATERIALS AND METHODS

Selenium Reagents and Cell Line. MSA was synthesized as described previously (7). Se-Met was purchased from Sigma (St. Louis, MO). The PC-3 human prostate cancer cells were obtained from American Type Culture Collection (Manassas, VA). The cells were cultured in RPMI 1640 supple-

Received 7/5/02; accepted 10/30/02.

The costs of publication of this article were defrayed in part by the payment of page charges. This article must therefore be hereby marked *advertisement* in accordance with 18 U.S.C. Section 1734 solely to indicate this fact.

¹ This work was supported by Grant CA 91990 from the National Cancer Institute, AACR-Cancer Research Foundation of America Fellowship in Prevention Research, Department of Defense Postdoctoral Fellowship Award, and was partially supported by core resources of the Roswell Park Cancer Institute Cancer Center support Grant P30 CA 16056 from the National Cancer Institute.

² To whom requests for reprints should be addressed, at Department of Cancer Prevention, Roswell Park Cancer Institute, Elm and Carlton Streets, Buffalo, NY 14263. Phone: (716) 845-8875; Fax: (716) 845-8100; E-mail: clement.ip@roswellpark.org.

³ The abbreviations used are: SELECT, Selenium and Vitamin E Chemoprevention Trial; MSA, methylseleninic acid; TUNEL, terminal deoxynucleotidyl transferase-mediated dUTP nick end labeling; PI, propidium iodide; GAPDH, glyceraldehyde-3-phosphate dehydrogenase; MTT, 3-(4,5-dimethylthiazol-2-yl)-2,5-diphenyltetrazolium bromide; TGF, transforming growth factor; RR, relative risk; BrdUrd, bromodeoxyuridine; Se-Met, selenomethionine; SOM, self-organizing map; MAPK, mitogen-activated protein kinase; PCNA, proliferating cell nuclear antigen.

mented with 10% fetal bovine serum, 100 units/ml penicillin, 100 $\mu\text{g}/\text{ml}$ streptomycin, and 2 mM glutamine, and maintained in an atmosphere of 5% CO_2 in a 37°C humidified incubator.

MTT Cell Proliferation Assay. The assay, which is based on the conversion of the yellow tetrazolium salt MTT to purple formazan crystals by metabolically active cells (11), provides a quantitative determination of viable cells. Cells were seeded in 24-well plates at a density designed to reach 70–80% confluency at the time of assay. At 48 h after seeding, cells were treated with various concentrations of Se-Met or MSA in triplicate. After 24, 48, or 72 h of treatment, 200 μl of MTT was added to each well of cells, and the plate was incubated for 4 h at 37°C. The MTT crystals from both attached and floating cells were solubilized in isopropanol and subjected to centrifugation to pellet the cellular debris. Spectrophotometric absorbance of each sample was measured at 570 nm using a Spectra Microplate Reader (SLT-Labstruments Ges.m.b.H., Salzburg, Austria).

Cell Cycle Analysis. PC-3 cells were plated at a density of 10^4 cells/cm² in T75 culture flasks and allowed to grow for 48 h to reach 70–80% confluency. Synchronization of cells was achieved by starving in serum-free medium for 48 h. Over 85% of cells were in G₀ phase at the end of this time period. On returning to regular growth medium for 6 h, cells were exposed to 10 μM MSA. The procedure of serum-starvation and refeeding has been described previously by Sinha and Medina (12) and Sinha *et al.* (13) to study the effect of selenium on cell cycling. After treatment for 24, 32, or 48 h, cells were trypsinized, washed in PBS, and fixed overnight in 70% ethanol at 4°C. The ethanol solution was subsequently removed after centrifugation, and cells were resuspended in a buffer containing 10 mM Tris (pH 7.5), 125 mM sucrose, 2.5 mM MgCl₂, 0.185% NP40, 0.02 mg/ml RNase A, 0.05% sodium citrate, and 25 $\mu\text{g}/\text{ml}$ PI. After incubation on ice for 1 h, cells were analyzed for DNA content using a FACScan cytometer (Becton Dickinson).

BrdUrd Labeling Assay. PC-3 cells were plated at a density of 10^4 cells/cm² in T75 culture flasks and synchronized as described above. On returning to regular growth medium for 6 h, cells were exposed to 10 μM MSA for 24 or for 48 h. During the last 30 min of MSA treatment, cells were labeled with 10 μM BrdUrd (10 μl of 1 mM BrdUrd was added to each ml of culture media). BrdUrd-labeled cells were trypsinized, fixed, treated with DNase I, and stained with FITC-conjugated anti-BrdUrd antibody using the BrdUrd Flow Kit from BD Pharmingen (San Diego, CA). Stained cells were then quantified by flow cytometry, and the data were analyzed with the WinList software (Variety Software House, Topsham, ME).

Quantitation of Apoptosis by Flow Cytometry. PC-3 cells were plated at a density of 10^4 cells/cm² in T175 culture flasks. At 48 h after seeding, cells were exposed to either 5 or 10 μM MSA for 48 or 72 h. Adherent cells harvested by mild trypsinization were pooled together with detached cells. Cells were stained with biotin-conjugated Annexin V, FITC-conjugated streptavidin, and PI using the Annexin V-Biotin Apoptosis Detection Kit (Oncogene Research Products, Boston, MA) as per the manufacturer's protocol. Apoptotic cells were subsequently counted by flow cytometry, and the data were analyzed with the WinList software (Variety Software House, Topsham, ME).

Oligonucleotide Array Analysis. PC-3 cells were plated at a density of 10^4 cells/cm² in 15-cm culture dishes. Synchronization was achieved as described above. After exposure to 10 μM MSA for 12, 24, 36, or 48 h, total RNA and protein were isolated using TRIzol (Life Technologies, Inc.). The experiment was repeated, and the total RNA collected from the replicate was pooled and submitted to microarray analysis using the U95A chip from Affymetrix (Santa Clara, CA). Biotinylated cRNA probe generation, as well as array hybridization, washing, and staining, was carried out according to the standard Affymetrix GeneChip protocol. Fluorescence intensity for each chip was captured with a Hewlett-Packard laser confocal scanner. Absolute analysis of each chip and comparative analysis of MSA-treated samples with the untreated control samples were performed by using the Affymetrix Microarray Suite software. The mean hybridization signal for each sample was set as 1000 arbitrary units to normalize the signal values of all of the genes on the chip (global normalization) between different samples. A treatment/control signal ratio of ≥ 2 or ≤ 0.5 was chosen as the criterion for induction or repression, respectively. These threshold values are commonly used in the literature for microarray expression analysis (14–16). GENECluster program (Massachusetts Institute of Technology, Boston, MA) and Affymetrix Data Mining Tool were used for clustering analysis.

Western Blot Analysis. Western blot analysis was performed as described previously (17) using the TRIzol isolated protein. Briefly, ~50 μg of protein was resolved over 10–15% SDS-PAGE and transferred to polyvinylidene difluoride membrane. The blot was blocked in blocking buffer [5% nonfat dry milk, 10 mM Tris (pH 7.5), 10 mM NaCl, and 0.1% Tween 20] overnight at 4°C, incubated with the primary antibody at 37°C for 1 h, followed by incubation with an antimouse antirabbit, or antisheep horseradish peroxidase-conjugated secondary antibody (Bio-Rad, Hercules, CA) at 37°C for 30 min. Individual protein bands were visualized by an enhanced chemiluminescence kit obtained from Amersham Pharmacia Biotech (Piscataway, NJ). Immunoreactive bands were quantitated by volume densitometry using the ImageQuant software (Molecular Dynamics, Sunnyvale, CA), and normalized to actin. The following monoclonal antibodies were used in this study (source): anti-actin (Sigma, St. Louis, MO); anti-DHFR, CDK1, and CDK2 (BD Transduction Laboratory, San Jose, CA); anti-PCNA (Santa Cruz Biotechnology, Santa Cruz, CA); and anti-cyclin A, cyclin E2, CDK4, p21^{WAF1} (NeoMarkers, Fremont, CA). Polyclonal antibodies to CHK2 and GADD153 were obtained from Calbiochem (La Jolla, CA) and Santa Cruz Biotechnology (Santa Cruz, CA), respectively.

Statistical Analysis. The Student's two-tailed *t* test was used to determine significant differences between treatment and control values, and *P* < 0.05 was considered statistically significant.

RESULTS

Sensitivity of Human Prostate Cancer Cells to MSA. The inhibitory effects of MSA and Se-Met on the accumulation of PC-3 cells were assessed by the MTT assay. As shown in Table 1, MSA was able to significantly suppress the growth of PC-3 cells in a time- and dose-dependent manner. At 72 h of treatment, 5 μM MSA reduced cell number by ~25%. Increasing the concentration of MSA to 10 μM resulted in a more pronounced effect, leading to a greater magnitude of growth inhibition in a shorter period of exposure. In contrast, a concentration of 200 or 400 μM Se-Met was required to produce significant decreases in cell number at 72 h or 48 h, respectively. It is thus evident that MSA is much more potent than Se-Met in inhibiting growth of these prostate cells.

Cell Cycle Block by MSA. To determine whether the decrease in cell number accumulation by MSA was related to cell cycle arrest, we proceeded to assess the evidence of cell cycle perturbation by flow cytometry of ethanol-permeabilized cells stained with PI. Synchronized PC-3 cells were treated with 10 μM MSA for 24, 32, or 48 h. MSA did not cause any significant change in cell cycle distribution (Fig. 1). However, flow cytometry of BrdUrd-labeled cells showed that MSA treatment resulted in a drastic decrease in the number of cells synthesizing DNA (Fig. 2). Therefore, the data suggest that MSA probably blocked cell cycle progression at multiple stages. It should be noted that flow cytometry of PI-stained cells would not be able to detect a change in the proportion of cells in different phases of the cell

Table 1 Effect of MSA or Se-Met on the accumulation of PC-3 cells at three treatment durations

Treatment	% of untreated control ^a		
	24 h	48 h	72 h
MSA (μM)			
1	97.0 \pm 3.5	98.9 \pm 5.0	99.0 \pm 4.9
2.5	107.2 \pm 5.0	106.4 \pm 3.8	101.8 \pm 6.2
5	104.2 \pm 5.0	103.7 \pm 5.3	74.2 \pm 6.5 ^b
10	101.6 \pm 6.3	46.3 \pm 4.4 ^b	38.4 \pm 1.7 ^b
Se-Met (μM)			
25	101.3 \pm 4.0	112.7 \pm 1.7	102.4 \pm 3.5
50	101.5 \pm 3.3	110.2 \pm 2.5	94.6 \pm 4.5
100	100.1 \pm 2.1	110.7 \pm 1.3	87.8 \pm 5.6 ^b
200	94.1 \pm 1.2	97.2 \pm 6.4	69.3 \pm 6.4 ^b
400	92.8 \pm 5.5	75.3 \pm 4.4 ^b	50.1 \pm 3.6 ^b

^a Results are expressed as mean \pm SE (*n* = 4 independent experiments).

^b Significantly different compared to the corresponding control value (*P* < 0.05).

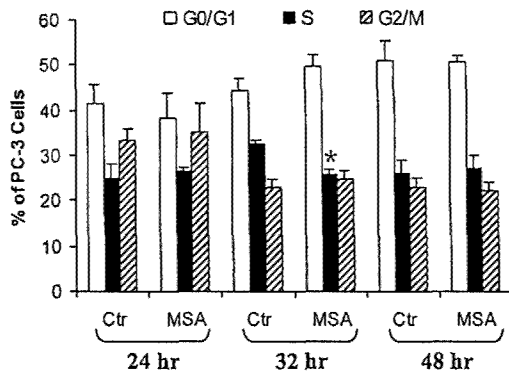


Fig. 1. Cell cycle distribution in PC-3 cells treated with MSA. Results are expressed as means \pm SE ($n = 3$). *, statistically significant ($P < 0.05$) versus untreated control.

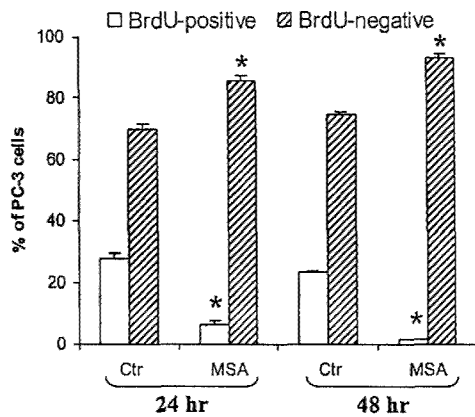


Fig. 2. BrdUrd (*BrdU*) labeling of PC-3 cells treated with MSA. Results are expressed as means \pm SE ($n = 3$). *, statistically significant ($P < 0.05$) versus untreated control.

cycle (*i.e.*, the percentage of cells in G_0 - G_1 , S phase, or G_2 -M) if there is a persistent slowdown in the transition in all phases of the cell cycle.

Induction of Apoptosis by MSA. In an attempt to determine whether MSA might also induce cell death, we incubated exponentially growing PC-3 cells for 48 or 72 h in the presence of 5 or 10 μ M MSA, and quantified the extent of apoptosis by flow cytometric analysis of cells labeled with annexin V and PI. Phosphatidylserine externalization is a characteristic of cells undergoing apoptosis. Annexin V has a strong affinity for phosphatidylserine. Staining cells simultaneously with annexin V and PI allows the resolution of intact cells (double negative), early apoptotic cells (annexin V-positive and PI-negative), and late apoptotic or necrotic cells (double positive), which can be located in the lower left, lower right, and upper right quadrants of the cytograms of Fig. 3A, respectively. Because only cells that are annexin V-positive and PI-negative are truly representative of apoptotic cells, the percentage of this cell population was quantitated from four individual experiments and shown in a bar graph form in Fig. 3B. MSA caused an induction of apoptosis at the 48-h time point, and the effect was maintained with longer exposure to MSA for 72 h. The increase of apoptosis, which followed the occurrence of growth arrest, appeared to maximize with 5 μ M MSA, and no further enhancement was detected with 10 μ M MSA.

Profiling of MSA-responsive Genes by Oligonucleotide Array Analysis. We used the Affymetrix human genome U95A Chip to profile the changes in gene expression and to characterize selenium-responsive targets that might lead to cell growth inhibition by MSA. This GeneChip contains probes to 12,000 known genes. As it would be more informative to do the profiling at a series of time points than

to do replicate analysis at a single time point, we decided to commit our available resources to the former design. For each time point at 12, 24, 36, and 48 h post-MSA, three separate preparations of RNA samples were pooled and submitted to array hybridization.

Pairwise comparative analysis between MSA-treated samples and the corresponding untreated control samples at each time point was performed by using the Affymetrix Microarray Suite software. This software determines whether a given gene is differently expressed based on a decision matrix including the net change in intensity values, fold of change, and other parameters. A no-change decision call was assigned a value of "1." Genes with expression changes of ≥ 2 or ≤ 0.5 were considered as MSA-responsive genes. The 2-fold difference limit was chosen based on our previous experience with microarray data analysis and was also in general agreement with other reported array experiments. Table 2 shows the number of genes induced or repressed by MSA at each time point. There were significantly fewer MSA-modulated genes at the 48-h time point than at the other three early time points. This could be because growth inhibition by MSA has reached $\sim 50\%$ at 48 h (Table 1) and because the underpinning molecular changes have already peaked and receded by this time.

To study in detail the kinetics of expression changes in response to

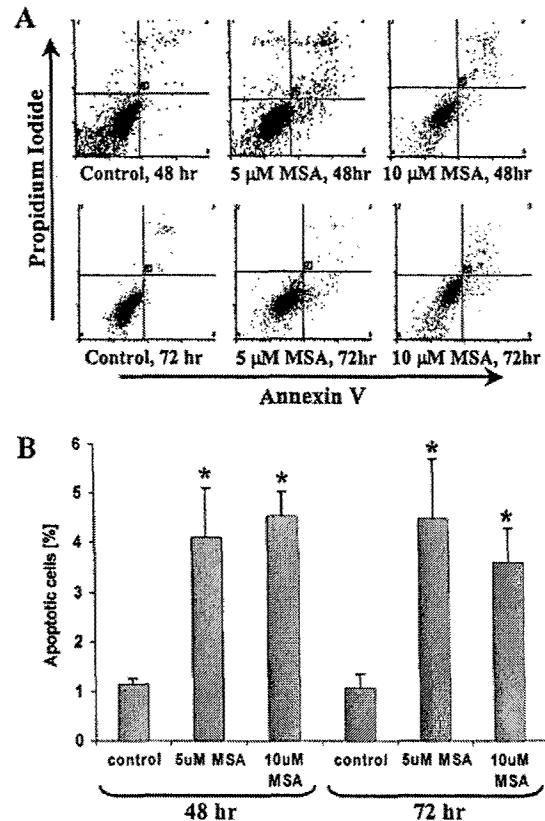


Fig. 3. Quantitation of apoptotic cells by flow cytometric analysis of MSA-treated PC-3 cells labeled with annexin V and PI. A, cytograms from flow cytometric analysis. Intact cells, early apoptotic cells, and late apoptotic and necrotic cells are located in the lower left, lower right, and upper right quadrants of the cytograms, respectively. B, percentages of early apoptotic cells. Data are presented as means \pm SE ($n = 4$). *, statistically significant ($P < 0.05$) versus untreated control.

Table 2. Number of genes modulated by MSA

Genes	Time point (h)			
	12	24	36	48
Induced by MSA	502	926	255	133
Repressed by MSA	364	496	588	136

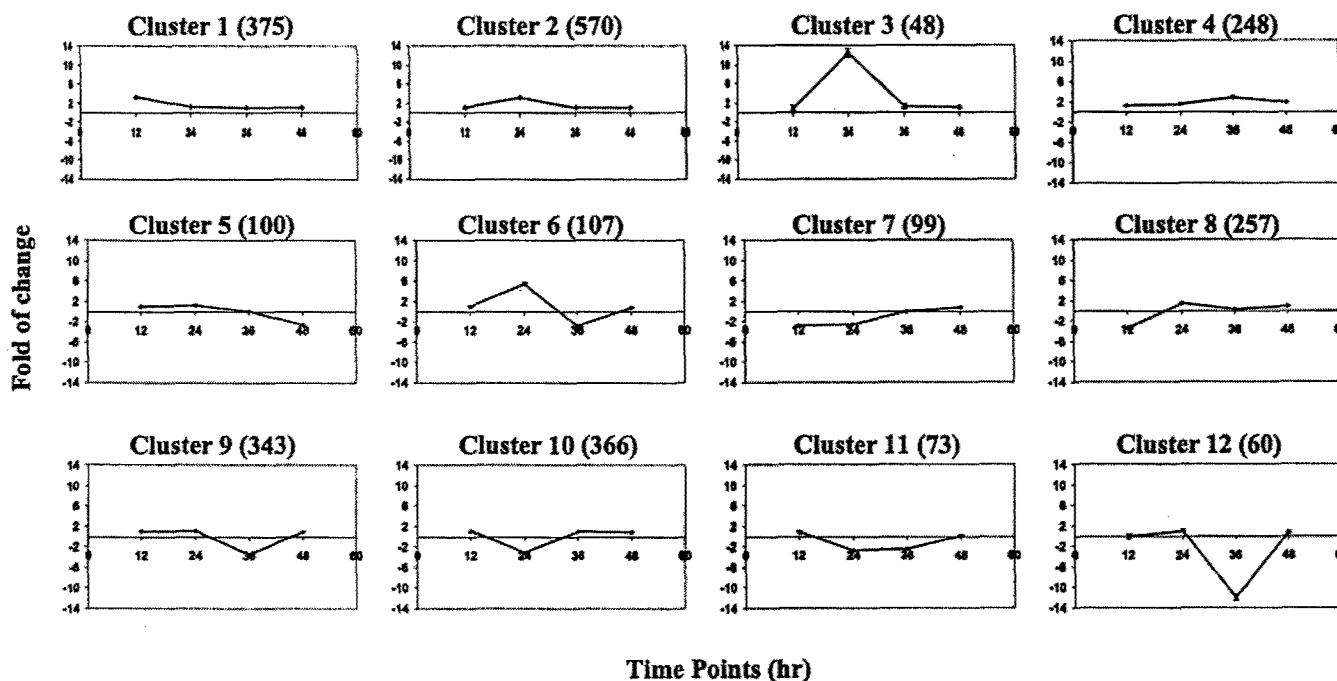


Fig. 4. Average gene expression profiles for each SOM cluster. The fold of change for each gene in a cluster was averaged and plotted against duration of treatment. Data are presented as means \pm SE. Numbers in parentheses, the number of genes included in each cluster. Twelve clusters were derived from the clustering analysis, demonstrating different kinetics of modulation by MSA.

MSA treatment, the genes modulated by MSA at one or more time points were subjected to clustering analysis using the SOM algorithm. Clustering analysis avails to the grouping of genes according to similarities in their expression profiles across multiple time points. The SOM algorithm is ideal for pattern discovery and has been found to be useful in the elucidation of biological pathways, because genes that are regulated in a coordinated fashion are often related. A total of 2647 genes were included in this analysis. This represents 21% of the genes on the U95A GeneChip. These genes fell into 12 clusters of distinct kinetics pattern of modulation by MSA (Fig. 4), with the early response genes in clusters 1, 7, and 8; the intermediate response genes in clusters 2, 3, 6, 10, and 11; and the late response genes in clusters 4, 5, 9, and 12. Because cell growth inhibition by 10 μ M MSA occurred between 24 to 48 h (Table 1), we consider the genes modulated by MSA at the 12-h time point as the early-response genes. We also believe that the change in expression of these early-response genes is important in initiating the cascade of events leading to the action of MSA. We, therefore, classify these early-response genes according to their known functions in cell growth/tumorigenesis (Table 3).

There is a prominent group of genes implicated in cell cycle regulation. Many negative cell cycle regulators were induced by MSA, including checkpoint proteins *RAD9* and *CHK2*, CDK inhibitors *p19^{INK4d}* and *p21^{WAF1}*, *RB-binding protein 1*, *GADD45*, and *protein phosphatase 2C*. On the other hand, numerous cyclins, CDKs, and genes required for DNA replication or mitosis were repressed by MSA. Because these genes control the transition of different phases of the cell cycle, the change in their expression could mediate the inhibitory effect of MSA on cell cycle progression. There is a second group of genes involved in apoptosis. Both *toll-like receptor 2* and *caspase 9* were up-regulated by MSA. *Toll-like receptor 2* is a death receptor (18), and *caspase 9* is an upstream activator of the caspase cascade (19). In addition, MSA down-regulated the expression of *survivin*, a member of the IAP (inhibitor of apoptosis) family. The reason that so few apoptosis-regulatory genes were affected by MSA at the 12-h time point is probably because the induction of apoptosis

by MSA did not become evident until after 48 h. An analysis of apoptosis gene expression changes at the 24- and 36-h time points will be the subject of a separate study.

In Table 3 is a group of genes encoding cytoskeleton components, cell membrane glycoproteins, as well as matrix metalloproteinases. The responses of cytoskeleton genes to MSA were varied. However, the up-regulation of invasion suppressors (e.g., *cadherins*) and the down-regulation of invasion activators (e.g., *integrins*, *endonexin*, hyaluronan receptors *CD44* and *RHAMM*, and *MMP21/22*) suggest a possible role of MSA in inhibiting tumor cell invasion. The table also shows a group of signal transduction genes that are responsive to MSA. In particular, there is a cluster of small GTPases and their associated factors, such as *Ras-like protein Tc10*, *GTPase activating factor-2*, *RAN-binding protein 8*, *G protein-coupled receptor 37*, *RAB31*, *RAB28*, *RAB7-like 1*, *regulator of G protein signaling 10*, *Rho E*, *Rho 2*, and *prenylated RAB acceptor 1*. These genes belong to the Ras and Rho family, the members of which are known to regulate diverse cellular functions, such as cell cycle progression, actin cytoskeleton organization, malignant transformation, and MAPK signaling cascades. In addition, MSA-mediated up-regulation of several MAPK cascade genes, including *MEK1*, *MEK3b*, *MEK5*, and *JNK1*, may amplify its effect on Ras/Rho signaling. Another noteworthy observation is the repression of a key player of the survival pathway, *PI3-kinase*. This suggests that selenium not only activates proapoptosis signals, but may also suppress survival signals to augment the stimulus to apoptosis.

MSA was found to modulate a large group of transcription factors, especially the zinc-finger family proteins (ZNFs), the myc proteins and associated factors, the ATF/CREB proteins and their binding proteins, as well as the inhibitor of DNA synthesis (Id) family proteins. Many of these transcription factors play critical roles in the regulation of cell cycle progression, apoptosis, and malignant transformation. The change in the expression of these *trans-acting* factors could lead to an altered transcription of a series of other genes. To wrap up the information summarized in Table 3, two growth factors

Table 3 Functional classification of MSA early-response genes

A value >1 represents induction; a value <1 represents repression.

Gene	Modulation
Cell cycle	
<i>RAD9</i>	3.0
<i>RB-binding protein 1</i>	2.0
<i>p19^{INK4d}</i>	2.0
<i>GADD45</i>	2.0
<i>p21^{WAF1}</i>	3.0
<i>PP2C-β</i>	4.0
<i>PP2C-α2</i>	2.0
<i>CHK2</i>	3.0
<i>CDC8</i>	0.6
<i>CDC7-related kinase</i>	0.5
<i>M phase phosphoprotein 1</i>	0.4
<i>ribonucleotide reductase M1 subunit</i>	0.4
<i>STK15</i>	0.5
<i>Mitotin</i>	0.5
<i>thymidylate synthase</i>	0.2
<i>chromatin assembly factor-1 p150 subunit</i>	0.5
<i>CDK1</i>	0.5
<i>MCM7</i>	0.3
<i>replication factor C</i>	0.4
<i>replication protein A 32-kDa subunit</i>	0.5
<i>dihydrofolate reductase (DHFR)</i>	0.2
<i>PCTAIRE-1</i>	0.3
<i>DNA pol-ε subunit B</i>	0.3
<i>DNA pol-α</i>	0.4
<i>protein phosphatase 2A regulatory subunit α</i>	0.2
<i>Cyclin A</i>	0.3
<i>Cyclin E2</i>	0.3
<i>MCM6</i>	0.5
<i>Ki67a</i>	0.2
<i>DNA primase</i>	0.4
<i>Kinesin-like 1</i>	0.2
<i>MCM3</i>	0.4
<i>Lamin B2</i>	0.4
<i>CDK4</i>	0.5
<i>MCM5</i>	0.2
<i>PCNA</i>	0.1
<i>CDK2</i>	0.5
Apoptosis	
<i>toll-like receptor 2</i>	2.6
<i>Caspase 9</i>	2.0
<i>Survivin</i>	0.3
Angiogenesis	
<i>VEGF-C</i>	0.4
Protein synthesis	
<i>eIF-4γ</i>	0.5
Growth factor	
<i>bFGF</i>	0.3
<i>Wnt7a</i>	0.3
Tumor suppressor/Growth inhibitor	
<i>BRCA2</i>	3.2
<i>DLC-1</i>	3.1
<i>TGF-β</i>	2.9
<i>TGF-β type III receptor</i>	3.6
<i>BMP-4</i>	4.8
<i>PTEN</i>	2.0
Transcription factor	
<i>BACH1</i>	2.2
<i>Hox5.4</i>	5.3
<i>ZNF345</i>	2.8
<i>ZNF217</i>	3.6
<i>ZNF165</i>	3.8
<i>ZNF267</i>	2.9
<i>ZNF75</i>	2.3
<i>Ring ZNF</i>	2.5
<i>ZNF274</i>	3.2
<i>ZNF278</i>	0.5
<i>ZNF X-linked</i>	0.3
<i>Kruppel-like ZNF</i>	3.5
<i>CBP/p300-interacting transactivation</i>	2.5
<i>CREB1</i>	3.0
<i>ATF5</i>	0.4
<i>E74-like factor 3</i>	2.4
<i>SRC1</i>	2.6
<i>Id1</i>	0.5
<i>Id3</i>	0.2
<i>Forkhead box M1B</i>	0.4
<i>N-myc interactor</i>	0.5
<i>Myc-associated ZNF</i>	0.2
<i>b-myb</i>	0.1
<i>Jun-B</i>	0.1

Table 3 Continued

Gene	Modulation
<i>HNF-3α</i>	0.5
<i>TAF170-α</i>	0.5
<i>NFκB p50</i>	0.2
<i>BAF57</i>	0.5
<i>HFH-11A</i>	0.4
<i>GADD153</i>	8.0
DNA repair	
<i>hPMS2</i>	6.0
<i>ERCC1</i>	3.3
Signal transduction	
<i>MEK1</i>	2.3
<i>MEK3b</i>	2.1
<i>MEK5</i>	6.0
<i>JNK1</i>	3.0
<i>Ras-like protein Tc10</i>	3.8
<i>GTPase activating factor-2</i>	4.4
<i>RAN-binding protein 8</i>	3.1
<i>G protein-coupled receptor 37</i>	2.3
<i>RAB31</i>	2.5
<i>RAB28</i>	2.1
<i>RAB7-like 1</i>	2.4
<i>Regulator of G protein signaling 10</i>	2.0
<i>Rho E</i>	3.2
<i>Rho 2</i>	0.5
<i>prenylated RAB acceptor 1</i>	0.4
<i>cAMP-regulated guanine nucleotide exchange factor II</i>	2.2
<i>CDP-DAG synthase</i>	2.3
<i>phospholipase C β4</i>	2.1
<i>receptor of retinoic acid</i>	5.0
<i>dual specificity phosphatase MKP-5</i>	6.4
<i>calmodulin-dependent protein kinase IV</i>	2.0
<i>PKC-α</i>	3.4
<i>PP1</i>	2.3
<i>PP5</i>	0.2
<i>PI 3-kinase</i>	0.4
Cytoskeleton	
<i>Adducin-γ</i>	2.4
<i>Calponin</i>	5.3
<i>Actin-binding protein 57</i>	11.9
<i>Cytokeratin 20</i>	4.1
<i>Tau</i>	0.2
<i>Filamin</i>	0.2
<i>Tubulin α 1 isoform 44</i>	0.4
<i>Non-muscle α-actinin</i>	0.4
Adhesion/Invasion	
<i>Cadherin-15</i>	6.5
<i>Cadherin-7</i>	2.5
<i>integrin β-5</i>	0.2
<i>integrin β-4</i>	0.3
<i>β 3-endonexin</i>	0.5
<i>CD44</i>	0.5
<i>RHAMM</i>	0.2
<i>MMP21/22</i>	0.1

(*bFGF* and *Wnt7a*), an angiogenesis molecule (*VEGF-C*), and one translation-initiation factor gene (*eIF-4γ*) that is amplified in cancer cells (20), were down-regulated by MSA. In contrast, three tumor suppressor genes (*BRCA2*, *DLC-1*, and *PTEN*), three TGF-β family members or receptor (*TGF-β*, *TGF-β type III receptor*, and *BMP-4*), and two DNA repair genes (*hPMS2* and *ERCC1*) were up-regulated by MSA. The regulation of these genes may represent additional mechanisms by which MSA exerts its anticancer effect.

Confirmation of Array Data. We used Western blot analysis to confirm the changes in expression of a subset of 10 cell cycle genes: *CHK2*, *p21^{WAF1}*, *GADD153*, *cyclin A*, *DHFR*, *CDK1*, *CDK2*, *CDK4*, *PCNA*, and *cyclin E2*. As shown in Fig. 5 and Table 4, the Western expression changes of 7 genes (*CHK2*, *p21^{WAF1}*, *GADD153*, *cyclin A*, *DHFR*, *CDK1*, and *CDK2*) correlated well with the array data. This represents an agreement rate of 70%. The lack of complete concordance could be attributable to either false positive signals of the array data or the discrepancy between transcript and protein expression. One noteworthy finding is that although both array and Western analyses showed a down-regulation of *CDK2* by MSA, the Western

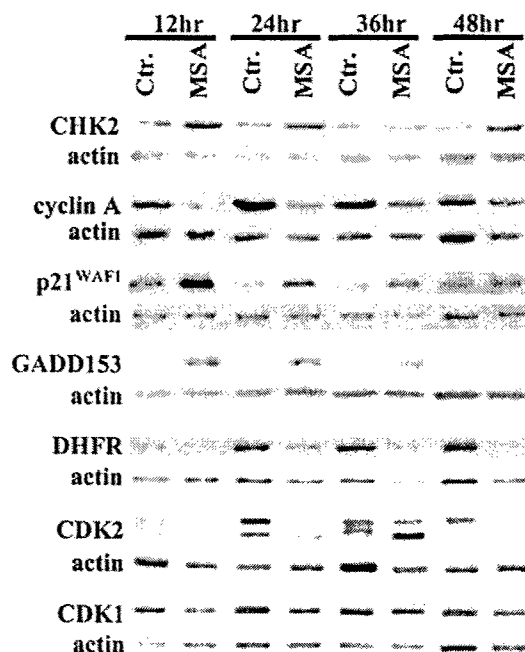


Fig. 5. Confirmation of array data by Western blot analysis. TRIzol-isolated proteins from PC-3 cells were subjected to immunoblotting using an antibody specific for CHK2, cyclin A, p21^{WAF1}, GADD153, DHFR, CDK2, or CDK1. Signals were normalized to the ones for actin to control for loading variation. The results shown here are representative of that from three similar independent experiments.

data additionally revealed a reduction of phosphorylated CDK2 (Fig. 5; Table 4). This dichotomy clearly reinforces a fundamental limitation of the array technology in that changes beyond the step of gene transcription are not detectable by this method.

DISCUSSION

Prostate cancer is the most common cancer diagnosed and the second leading cause of cancer-related deaths in men in the United States. However, little is known about the etiological factors for this disease. Consequently, it is not possible to institute primary intervention strategies to remove the causative agents from the environment. Secondary intervention strategies are, therefore, necessary to reduce the morbidity and mortality of prostate cancer, and selenium intervention has been championed as a viable option. The present study was undertaken to investigate the molecular targets and the signaling pathways underlying the anticancer activity of selenium in prostate.

Previous studies by Sinha and Medina and by Sinha *et al.* (12, 13) showed that selenium is able to block cell cycle progression at specific checkpoints, which might be explained by a decrease in CDK2 kinase

activity. These experiments were done with mouse mammary tumor cells treated with 50 μM of methylselenocysteine; this concentration of selenium is at least 10 times higher than that found in the circulation under normal physiological condition. For this reason, MSA is a more appropriate agent for *in vitro* studies. Our results demonstrate that MSA inhibits the growth of prostate cancer cells by cell cycle blockade and apoptosis. We used the GeneChip technology to profile selenium-mediated gene expression changes in a time course experiment. Of a total of 12,000 genes screened, over 2,500 were identified to be responsive to selenium treatment. The sheer magnitude of this number is somewhat unexpected. These genes were grouped into early-, intermediate-, and late-response clusters. Because the early-response genes are likely to be more important in initiating the effects of selenium, we focused our attention on them in our follow-up analysis.

Certain key cell cycle regulators are among the early-response genes. On the basis of their altered expression, we propose a number of tentative signaling pathways (in a cartoon format) that might mediate the outcome of cell cycle blockade by selenium. As shown in Fig. 6, selenium treatment increases the expression of p21^{WAF1}, which has dual functions in regulating the activity of CDK/cyclin complexes. Although p21^{WAF1} is a potent inhibitor of cyclin E/A-dependent CDK1/2, it promotes the assembly and the nuclear translocation of cyclin D-CDK4/6 complexes, leading to an increase in cyclin D-associated kinase activity (21). However, the induction of p19^{INK4d} by selenium counteracts the latter effect. The p19^{INK4d} protein binds to and inhibits the cyclin D-CDK4/6 complexes, thus releasing p21^{WAF1} from CDK4 and CDK6. The cooperative action of p19^{INK4d} and p21^{WAF1} leads ultimately to an inhibition of both cyclin D- and cyclin A/E-dependent kinases. The down-regulation of CDK1, CDK2 and cyclin A by selenium provides an amplified effect on this cascade of events. Complete phosphorylation/inactivation of pRB requires the sequential actions of cyclin D-CDK4/6 and cyclin E-CDK2 (22). Thus, p19^{INK4d}- and p21^{WAF1}-mediated inhibition of CDK2, CDK4, and CDK6 could result in decreased phosphorylation of pRB. Hypophosphorylated pRB interacts with, and negatively regulates, the activity of E2F transcription factors. Loss of E2F activity prevents the transcription of genes, *e.g.*, *DHFR* and *cyclin A*, required for progression into S phase. In addition, although not depicted in Fig. 6, p21^{WAF1} is able to bind to PCNA and directly inhibit its activity (23), and interact with E2F subunits and disrupt E2F-CDK-p107 DNA binding complex (24, 25). These changes, collectively, are expected to result in a blockade of DNA replication.

As shown in Fig. 7, the elevated expression of CHK2 by selenium treatment leads to increased phosphorylation of CDC25 proteins, which subsequently bind to 14-3-3 proteins and are exported to the cytoplasm. CDC25 proteins are responsible for removing the inhibitory phosphates from CDK1 and CDK2, allowing them to be activated

Table 4 Comparison of expression changes detected by array and Western analyses

The values represent treatment:control ratio.

Gene	Array analysis					Western analysis ^a				
	12 h	24 h	36 h	48 h	Diff Call ^b	12 h	24 h	36 h	48 h	Diff Call
<i>CHK2</i>	3	1	1	1	↑	3	4	1	10	↑
<i>p21^{WAF1}</i>	3	1	1	1	↑	3	5	4	3	↑
<i>GADD153</i>	8	12	6	2	↑	14	6	8	1	↑
<i>cyclin A</i>	0.3	1	0.3	0.4	↓	0.3	0.3	0.4	1	↓
<i>DHFR</i>	0.25	1	0.5	1	↓	0.3	0.3	0.3	0.2	↓
<i>CDK1</i>	0.5	0.5	1	1	↓	0.3	0.7	1	1	↓
<i>CDK2</i>										
Phosphorylated	0.5	1	1	1	↓	0.4	0.06	0.6	0.09	↓
Unphosphorylated						0.3	0.3	10	0.8	↓

^a The value represents the mean of three experiments. The SE is about 10%.

^b Diff Call, difference call; ↑, increase; ↓, decrease.

congruency, however, is highlighted against a backdrop of certain differences in cell genotype and methodological issues. The PC-3 human prostate cancer cells are null for p53, whereas the premalignant MCF10AT human breast cells have a functional p53, suggesting that p53 is not required for the action of selenium. The 12,000-gene oligonucleotide GeneChip was used in the prostate cell study, whereas the 200-gene membrane-based cDNA array was used in the breast cell study. Despite these differences, similar selenium targets were identified, including GADD153, cyclin A, CDK1, CDK2, CDK4, CDC25, E2Fs, as well as the MAPK/JNK and phosphoinositide-3 kinase pathways, thus lending confidence to the array data. Previous studies of gene expression changes in response to selenium have generally been limited to the analysis of a few or a subset of genes and, therefore, have provided only a very narrow view of the entire landscape. As far as we are aware of, this is the most comprehensive gene expression profiling study on the molecular mechanism of selenium in chemoprevention.

Venkateswaran *et al.* (37) recently reported that PC-3 cells are not growth inhibited by Se-Met unless they are transfected with a functional androgen receptor. Suffice it to point out that the sensitivity of PC-3 and another androgen-independent prostate cancer cell line, DU-145, to Se-Met has been documented by two other groups of investigators (38, 39). Furthermore, Jiang *et al.* (9) showed that DU-145 cells can be induced to undergo apoptosis by MSA at physiological concentrations. Together with our study, the weight of evidence seems to favor the notion that the responsiveness of prostate cancer cells to selenium is not dependent on the presence of a functional androgen receptor. Although androgen plays a critical role in prostate carcinogenesis, a significant proportion of prostate cancers eventually become androgen-unresponsive and refractory to hormonal therapy. The fact that androgen-unresponsive cells are sensitive to selenium-induced growth inhibition is encouraging because it suggests that selenium intervention may be a viable strategy for preventing prostate cancer recurrence after prostatectomy.

ACKNOWLEDGMENTS

We are grateful to Dorothy Donovan, Tamora Loftus, Todd Parsons, Rita Pawlak, Cathy Russin, and Janice Hoffmann for their excellent technical assistance.

REFERENCES

- Clark, L. C., Combs, G. F., Jr., Turnbull, B. W., Slate, E. H., Chalker, D. K., Chow, J., Davis, L. S., Glover, R. A., Graham, G. F., Gross, E. G., Krongrad, A., Leshner, J. L., Jr., Park, H. K., Sanders, B. B., Jr., Smith, C. L., and Taylor, J. R. Effects of selenium supplementation for cancer prevention in patients with carcinoma of the skin. A randomized controlled trial. Nutritional Prevention of Cancer Study Group. *J. Am. Med. Assoc.*, 276: 1957-1963, 1996.
- Hoque, A., Albanes, D., Lippman, S. M., Spitz, M. R., Taylor, P. R., Klein, E. A., Thompson, I. M., Goodman, P., Stanford, J. L., Crowley, J. J., Coltman, C. A., and Santella, R. M. Molecular epidemiologic studies within the selenium and vitamin E cancer prevention trial (SELECT). *Cancer Causes Control*, 12: 627-633, 2001.
- Ip, C. Differential effect of dietary methionine on the biopotency of selenomethionine and selenite in cancer chemoprevention. *J. Natl. Cancer Inst. (Bethesda)*, 80: 258-262, 1988.
- Ip, C., and Hayes, C. Tissue selenium levels in selenium-supplemented rats and their relevance in mammary cancer protection. *Carcinogenesis (Lond.)*, 10: 921-925, 1989.
- Ip, C., and Ganther, H. E. Activity of methylated forms of selenium in cancer prevention. *Cancer Res.*, 50: 1206-1211, 1990.
- Ip, C., Hayes, C., Budnick, R. M., and Ganther, H. E. Chemical form of selenium, critical metabolites, and cancer prevention. *Cancer Res.*, 51: 595-600, 1991.
- Ip, C., Thompson, H. J., Zhu, Z., and Ganther, H. E. *In vitro* and *in vivo* studies of methylseleninic acid: evidence that a monomethylated selenium metabolite is critical for cancer chemoprevention. *Cancer Res.*, 60: 2882-2886, 2000.
- Dong, Y., Ganther, H. E., Stewart, C., and Ip, C. Identification of molecular targets associated with selenium-induced growth inhibition in human breast cells using cDNA microarrays. *Cancer Res.*, 62: 708-714, 2002.
- Jiang, C., Wang, Z., Ganther, H., and Lu, J. Caspases as key effectors of methyl selenium-induced apoptosis (anoikis) of DU-145 prostate cancer cells. *Cancer Res.*, 61: 3062-3070, 2001.
- Sinha, R., Unni, E., Ganther, H. E., and Medina, D. Methylseleninic acid, a potent growth inhibitor of synchronized mouse mammary epithelial tumor cells *in vitro*. *Biochem. Pharmacol.*, 61: 311-317, 2001.
- Vistica, D. T., Skehan, P., Scudiero, D., Monks, A., Pittman, A., and Boyd, M. R. Tetrazolium-based assays for cellular viability: a critical examination of selected parameters affecting formazan production. *Cancer Res.*, 51: 2515-2520, 1991.
- Sinha, R., and Medina, D. Inhibition of cdk2 kinase activity by methylselenocysteine in synchronized mouse mammary epithelial tumor cells. *Carcinogenesis (Lond.)*, 18: 1541-1547, 1997.
- Sinha, R., Kiley, S. C., Lu, J. X., Thompson, H. J., Moraes, R., Jaken, S., and Medina, D. Effects of methylselenocysteine on PKC activity, cdk2 phosphorylation and *gadd* gene expression in synchronized mouse mammary epithelial tumor cells. *Cancer Lett.*, 146: 135-145, 1999.
- Wang, Y., Rea, T., Bian, J., Gray, S., and Sun, Y. Identification of the genes responsive to etoposide-induced apoptosis: application of DNA chip technology. *FEBS Lett.*, 445: 269-273, 1999.
- Kaminski, N., Allard, J. D., Pittet, J. F., Zuo, F., Griffiths, M. J. D., Morris, D., Huang, X., Sheppard, D., and Heller, R. A. Global analysis of gene expression in pulmonary fibrosis reveals distinct programs regulating lung inflammation and fibrosis. *Proc. Natl. Acad. Sci. USA*, 97: 1778-1783, 2000.
- Chen, C.-R., Kang, Y., and Massague, J. Defective repression of c-myc in breast cancer cells. *Proc. Natl. Acad. Sci. USA*, 98: 992-999, 2001.
- Dong, Y., Asch, H. L., Medina, D., Ip, C., Ip, M., Guzman, R., and Asch, B. B. Concurrent deregulation of gelsolin and cyclin D1 in the majority of human and rodent breast cancers. *Int. J. Cancer*, 81: 930-938, 1999.
- Aliprantis, A. O., Yang, R. B., Weiss, D. S., Godowski, P., and Zychlinsky, A. The apoptotic signaling pathway activated by Toll-like receptor-2. *EMBO J.*, 19: 3325-3336, 2000.
- Kuida, K., Haydar, T. F., Kuan, C. Y., Gu, Y., Taya, C., Karasuyama, H., Su, M. S., Rakic, P., and Flavell, R. A. Reduced apoptosis and cytochrome c-mediated caspase activation in mice lacking caspase 9. *Cell*, 94: 325-337, 1998.
- Brass, N., Heckel, D., Sahin, U., Pfreundschuh, M., Sybrecht, G. W., and Meese, E. Translation initiation factor eIF-4 γ is encoded by an amplified gene and induces an immune response in squamous cell lung carcinoma. *Hum. Mol. Genet.*, 6: 33-39, 1997.
- Sherr, C. J., and Roberts, J. M. CDK inhibitors: positive and negative regulators of G₁-phase progression. *Genes Dev.*, 13: 1501-1512, 1999.
- Lundberg, A. S., and Weinberg, R. A. Functional inactivation of the retinoblastoma protein requires sequential modification by at least two distinct cyclin-cdk complexes. *Mol. Cell. Biol.*, 18: 753-761, 1998.
- Waga, S., Hannon, G. J., Beach, D., and Stillman, B. The p21 inhibitor of cyclin-dependent kinases controls DNA replication by interaction with PCNA. *Nature (Lond.)*, 369: 574-578, 1994.
- Delavaine, L., and La Thangue, N. B. Control of E2F activity by p21/Waf1/Cip1. *Oncogene*, 18: 5381-5392, 1999.
- Dimri, G. P., Nakanishi, M., Desprez, P. Y., Smith, J. R., and Campisi, J. Inhibition of E2F activity by the cyclin-dependent protein kinase inhibitor p21 in cells expressing or lacking a functional retinoblastoma protein. *Mol. Cell. Biol.*, 16: 2987-2997, 1996.
- Falck, J., Mailand, N., Syljuasen, R. G., Bartek, J., and Lukas, J. The ATM-Chk2-Cdc25A checkpoint pathway guards against radioresistant DNA synthesis. *Nature (Lond.)*, 410: 842-847, 2001.
- Matsuoka, S., Huang, M., and Elledge, S. J. Linkage of ATM to cell cycle regulation by the Chk2 protein kinase. *Science (Wash. DC)*, 282: 1893-1897, 1998.
- Abcouwer, S. F., Schwarz, C., and Meguid, R. A. Glutamine deprivation induces the expression of GADD45 and GADD153 primarily by mRNA stabilization. *J. Biol. Chem.*, 274: 28645-28651, 1999.
- Choi, A. M., Fargnoli, J., Carlson, S. G., and Holbrook, N. J. Cell growth inhibition by prostaglandin A₂ results in elevated expression of *gadd153* mRNA. *Exp. Cell Res.*, 199: 85-89, 1992.
- Eymin, B., Dubrez, L., Allouche, M., and Solary, E. Increased *gadd153* messenger RNA level is associated with apoptosis in human leukemic cells treated with etoposide. *Cancer Res.*, 57: 686-695, 1997.
- Guyton, K. Z., Xu, Q., and Holbrook, N. J. Induction of the mammalian stress response gene *GADD153* by oxidative stress: role of AP-1 element. *Biochem. J.*, 314(Pt 2): 547-554, 1996.
- Jeong, J. K., Huang, Q., Lau, S. S., and Monks, T. J. The response of renal tubular epithelial cells to physiologically and chemically induced growth arrest. *J. Biol. Chem.*, 272: 7511-7518, 1997.
- Johnsson, A., Strand, C., and Los, G. Expression of GADD153 in tumor cells and stromal cells from xenografted tumors in nude mice treated with cisplatin: correlations with cisplatin-DNA adducts. *Cancer Chemother. Pharmacol.*, 43: 348-352, 1999.
- Kim, R., Oh, Y., Inoue, H., and Toge, T. Taxotere activates transcription factor AP-1 in association with apoptotic cell death in gastric cancer cell lines. *Anticancer Res.*, 19: 5399-5405, 1999.
- Luethy, J. D., and Holbrook, N. J. Activation of the *gadd153* promoter by genotoxic agents: a rapid and specific response to DNA damage. *Cancer Res.*, 52: 5-10, 1992.
- Zinszner, H., Kuroda, M., Wang, X., Batchvarova, N., Lightfoot, R. T., Remotti, H., Stevens, J. L., and Ron, D. CHOP is implicated in programmed cell death in response to impaired function of the endoplasmic reticulum. *Genes Dev.*, 12: 982-995, 1998.
- Venkateswaran, V., Klotz, L. H., and Fleshner, N. E. Selenium modulation of cell proliferation and cell cycle biomarkers in human prostate carcinoma cell lines. *Cancer Res.*, 62: 2540-2545, 2002.
- Menter, D. G., Sabichi, A. L., and Lippman, S. M. Selenium effects on prostate cell growth. *Cancer Epidemiol. Biomark. Prev.*, 9: 1171-1182, 2000.
- Redman, C., Scott, J. A., Baines, A. T., Basye, J. L., Clark, L. C., Calley, C., Roe, D., Payne, C. M., and Nelson, M. A. Inhibitory effect of selenomethionine on the growth of three selected human tumor cell lines. *Cancer Lett.*, 125: 103-110, 1998.